Design of energy-saving driver circuit for 80 Watt LED using Flyback Converter

DOI : 10.36909/jer.ICMET.17199

Rajesh Narayan Deo**, Ashish Shrivastava*, Kalyan Chatterjee**

**Department of Electrical Engineering, Indian Institute of Technology (ISM), Dhanbad, Jharkhand, 826004, India.

*Department of Electrical Engineering, Manipal University Jaipur, Rajasthan, 303007, India.

* Corresponding Author: rewa.ashish@gmail.com

ABSTRACT

Due to numerous features such as compact size, longevity, mercury-free start, and higher color rendering index, the introduction of light-emitting diode (LED) lights has changed residential and commercial lighting systems worldwide. There are two main types of LED driver configurations: single-stage (SS) and double-stage (DS). Low-power systems employ SS configuration converters, while high-power commercial systems use DS configuration converters. This study presented a discontinuous conduction mode (DCM) flyback converter with a PI controller for LED lighting, replacing double-stage converter systems. The proposed DCM-based flyback AC-DC converter includes fewer components, lower total harmonic distortions (THD), improved power factor, and high efficiency. The hardware prototype was created and tested at various AC main voltages to ensure the feasibility of the proposed model. At rated voltage 230 V, system THD is 5.2 %, power factor is 0.995, and efficiency is 92.1 %. The whole system efficiency meets the Energy Star standards.

Keywords: PFC, LED Lighting, DC-DC Converter, Power Quality.

INTRODUCTION

Solid-state lighting (SSL), commonly known as the light-emitting diode (LED), was introduced in 1970. Despite being just a decade old, this technology has proven to be better than traditional lighting systems. Furthermore, when compared to traditional sources, it is simple to use and attracted much interest due to several benefits such as lightweight, compact size, high luminous efficiency, energy savings, prolonged lifetime, and availability in various colours (Y. Wang, et al., 2017). LEDs used for commercial purposes (office and shopping mall lighting; interior decoration and street lighting etc.) commonly have 10 to 200 Watts of output power with high luminous efficiency, more than 50,000 hours of service life, mercury-free content, less emission of carbon dioxide, low response time, negligible pollution and approved stability (Fonseca, et al., 2017, Agrawal, et al., 2018, C. Y. Wu, et al., 2008). These devices satisfy the Energy Star standards C-type lighting devices with THD less than 15% and PF about 0.9 compared to conventional lighting sources (Choi, et al., 2005, Y. Li, et al., 2018, Henao, et al., 2017). When designing control circuitry for high-power LED lighting, four critical variables are to be considered: stability, electrical effectiveness, cost-effectiveness, and energy economy. In non-isolated converters, LED modules are replaced without disconnecting the main source. Hence put human safety at risk. In such instances, the driver output must be isolated. A transformer is typically employed to provide isolation between LED outputs and the transformer input. As a result, an isolated driver is suitable for use without the risk of electrical shock. Another key advantage of this transformer is that any disturbance at input side is not directly communicated to the output side, ensuring that the output LEDs are protected from transient and surge occurrences on the AC source. Two types of structure for outdoor lighting are preferred, which drives the LEDs optimally. These are single-stage (SS) configurations and double-stage (DS) configurations. The DS configuration works in two stages. In the first stage, the AC-DC converter is used along with PFC, and in the second stage, the DC-DC converter is used to control either output current or output voltage (Rico-Secades, et al., 2005, Lin, et al., 2014). Double-stage power configuration is opted for large power system due to its optimal control characteristic. But, in this configuration, current ripples generate undesirable invisible

flashing. DS configuration has a higher cost and lower efficiency due to its complex structure. And due to the high voltage across the power factor corrected circuit, the reliability and life span of the DC-link capacitor diminishes. Hence, single-stage configuration converters are usually used for low-power LED lighting applications due to the above limitations. Single-Stage (SS) converters are primarily applied in low power applications due to its simple configuration and cost-effectiveness. The SS configuration incorporates a combined DC-DC converter and a power factor corrected (PFC) circuit (B. Singh, et al., 2003, Singh, B., et al., 2011, Deo. Rajesh, et al., 2019). A single-stage flyback converter for low-power LEDs is preferred because it shows good power quality (PQ) parameters. It has low THD, good efficiency, high power factor, and does not require an inductive filter at the output side because the flyback transformer acts as an output filter. And also, this transformer isolates the input and output stages (Zheng; et al., 2006, Cheng, et al., 2015). The flyback converter is the most frequently recognized isolated converter among the single-stage DC-DC topologies for LED drivers. Compared to other DC-DC converters, the flyback converter provides several advantages (Chou, et al., 2013, Zhang, et al., 2012, Xie, et al., 2012). A single switch flyback converter is easy to design, has fewer components, takes up less space, and is more cost-effective. And its output voltage is changed by adjusting the turns ratio of the transformer. The output load voltage of the flyback converter can be controlled by governing the switching action of the pulses given to MOSFET in the flyback converters, which is generally attained through linear controllers (Hwang, et al., 2012, Hsieh, et al., 2013). Since these controllers are designed by linearizing the flyback converter model and thus operating point is over an absolute linearized set of points This paper describes a flyback converter with a discontinuous conduction mode (DCM) for an 80-Watt LED load. It uses a DCM-based SS flyback with a PI controller, where only one sensing element is required, i.e., output voltage with reduced cost

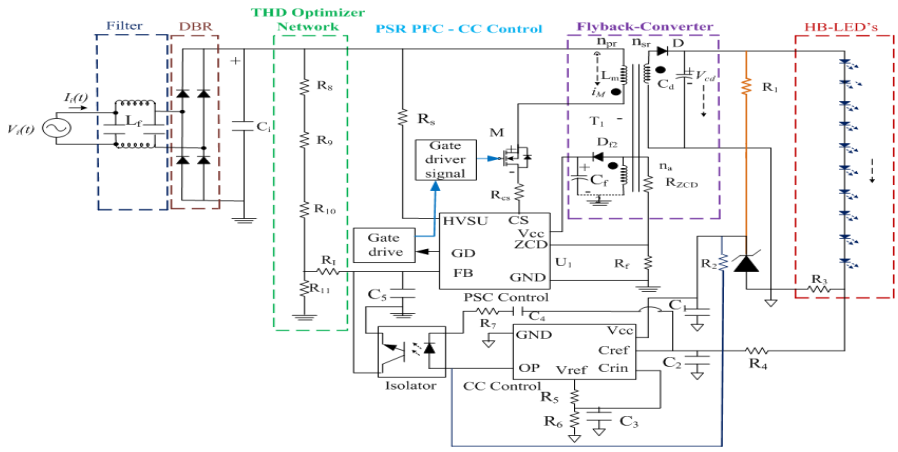

Figure 1. Flyback converter in DCM mode

and improved power quality (PQ). A prototype of 80-Watt flyback converter is developed in Laboratory. The study investigated and discusses the feasibility of the proposed flyback-based LED driver and its controller.

FUNDAMENTAL OPERATION SS FLYBACK CONVERTER

The single-stage flyback configuration converter isolates the rectifier and LED load shown in figure 1 and operates in discontinuous conduction mode (DCM). uses n-channel MOSFET. Throughout the analysis, MOSFET and diode are considered ideal. V_d represents rectified voltage of input supply voltage. L_m represents the magnetizing inductance of the converter transformer. During ON State of Switch M, energy is stored across L_m, and during OFF state of the power switch, energy is stored in flyback secondary winding of the transformer. A bulk electrolytic capacitor (C_d) is an energy-storing element that provides ripple-free DC voltage to the LED load. Depending on the inductor current continuity of the primary side of the transformer, the SS flyback converter can work in continuous, discontinuous, or boundary conduction mode. Switching frequency (M) is very high, producing pulsating waveform at input

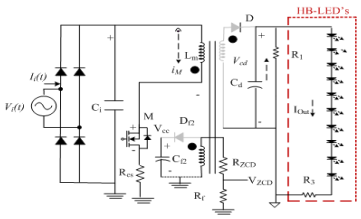

Figure 2. Mode I Operation

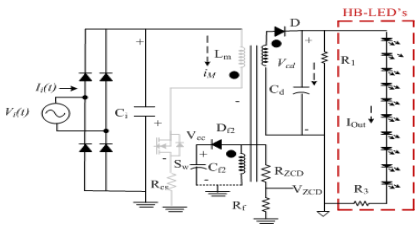

Figure 3. Mode II Operation

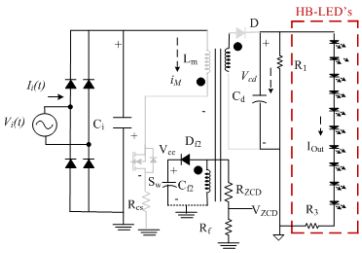

Figure 4. Mode III Operation

line current. Controlling magnitude and degree of current fluctuation can produce a line current that is in phase with the line voltage. As a consequence, at the input side, THD is decreased and nearly unit PF is achieved. Furthermore, Figures 2–4 demonstrate the operation of the SS flyback converter topology, which is divided into three stages/modes.

I-Mode: The M switch is turned on in this converter stage, and a diode is turned off. The input energy is stored in the flyback transformer on the input side, as seen in Figure 2. The rectified voltage across the converter can be calculated as follows:

$$V_d = |V_i(t)| = |V_{mx} \sin(\omega_{ag} t)| \tag{1}$$

Where V_{mx} , ω_{ag} are the maximum supply voltage and input angular frequency. During this mode of operation, current across the primary side increases linearly and given by:

$$i_{L_m}(t) = \frac{V_m}{L_m} |\sin(2\pi f_l t)| (t - t_o^{'}) \tag{2}$$

And maximum current across the primary side of an inductor is calculated by:

$$i_{L_{mp}}(t) = \frac{V_m}{L_m} |\sin(2\pi f_l t)| (t_1^{'}) \tag{3}$$

II-Mode: During this mode of operation, the switch is opened. Polarity across the secondary side of the transformer is changed. Due to this, the diode conducts. And energy stored in the secondary winding of a transformer is transferred to the LED load through the capacitor present at the output side. The primary side current decreases to zero, and secondary current flows through diode and load, and its circuit diagram is depicted in Figure 3. V_{out} is the output voltage of the converter. Hence the primary winding voltage in this mode of operation is calculated by:

$$V_{sr} = \frac{V_{pr}}{n} = \frac{V_{out}}{n} \tag{4}$$

And magnetizing inductor current, which decreases linearly during this stage, is given by:

$$i_{L_m}(t) = \frac{V_m \left|\sin(2\pi f_l t)\right| - \frac{V_{out}}{n}}{L_m}(t - t_1') + i_{L_{mp}} \tag{5}$$

III-Mode: During this mode of operation, both power switch (M) and power diode (D) is in OFF state, and only load current flows across the load through the capacitor, and its circuit diagram is depicted in figure 4.

DESIGN CONSIDERATIONS

The design of a single-stage PFC converter is presented in this section. The LED driver is mainly composed of the selection and design characteristics of individual components of the selected PFC converter. The front-end PFC converter is designed for a 60-110V DC streetlight LED module with a constant LED current of 700mA. The voltage appearing before the DBR is given as,

$$V_i(t) = V_{mx} Sin(\omega_{ag} t) = \sqrt{2} 220 Sin(2\pi 50 t) = \sqrt{2} 220 Sin(314t) = 311 Sin(314t) \tag{6}$$

V_{mx} is the maximum supply voltage value, and ω_{ag} is the line frequency in rad/sec.

The input voltage that appears after the DBR is denoted as V_d and given as,

$$V_d = \left|V_i(t)\right| = \left|V_{mx} Sin(\omega_{ag} t)\right| = \left|311 Sin(314t)\right| \tag{7}$$

Where, | | denotes the modulus function. The V_{dc} for flyback PFC converters is calculated as,

$$V_{dc} = \frac{D}{(1 - D)} \frac{N_{sr}}{N_{pr}} V_d \tag{8}$$

D, N_{sr}, N_{pr} represent the duty cycle, secondary turns, and primary turns, respectively.

D is the duty cycle of an isolated PFC converter and given as,

$$D = \frac{V_{dc} n}{V_d + V_{dc} n} = \frac{V_{dc} n}{\left| V_{mx} Sin\left(V_{ag} \right) \right| \quad _{dc} n} \tag{9}$$

The turn ratio in terms of input/output voltage and duty cycle is given by;

$$\frac{N_p}{N_s} = \frac{D}{(1 - D) V_{dc}} V_d = \frac{V_R}{V_{dc}} = \frac{150}{120} = 1.25$$

(10)

V_R is the equivalent voltage reflection desired from the input and duty cycle. This voltage is used as a trade-off for efficiency and the absolute voltage on the active PFC converter switch. The high value of V_R is responsible for low switching loss at this voltage; however, more voltage spike is possible at the drain of PFC MOSFET. It is calculated after putting reflection voltage 150V and output DC voltage 120V. This converter works on peak current mode, so the transformer's primary winding current is limited to peak value. The value can be set by the user depending on the trade-off of switching and conduction loss. Eq. (11) shows the peak current;

$$I_{pr} = \frac{V_{CS}}{R_{CS}} = \frac{0.7}{0.4} = 1.75A$$

(11)

Where, V_{CS} and R_{CS} are controller sinking voltage and current sense resistor value.

Flyback Transformer Design

The design selection of a high-frequency transformer is based on calculating the number of turns (primary, secondary and auxiliary), core selection, and winding wire gauge selection. The ferrite core selected for this power level design is ETD34/17/11 or equivalent similar geometry core commercially available in the market. The primary number of turns is selected as,

$$N_p = \frac{V_{dc(\max)} \mathrm{D}_{\min}}{A_c B_m f_s} = \frac{424 * 0.3}{91.6 * 10^{-6} * 0.25 * 65000} = 85 \tag{12}$$

$V_{dc(max)}$, D_{min}, A_c, B_m, and f_s are maximum DC input voltage, minimum duty cycle, core area, maximum flux density (0.25T), and converter switching frequency. The primary number of turns is selected considering 300VAC input equivalent maximum DC voltage (424V), minimum duty cycle 0.3 (using Eq. 9), core area A_c (91.6mm^2), and switching frequency 65 kHz. The secondary winding turns is calculated using Eqn. (13) turn ratio (1.25). The primary winding RMS current is calculated as Eqn. (13) using Eqn. 10 and Eqn.13 as follows;

$$I_{p(rms)} = \frac{I_p \sqrt{D_{\max}}}{\sqrt{3}} = \frac{1.75\sqrt{0.5}}{\sqrt{3}} = 0.71A \tag{13}$$

The wire area calculation for primary winding is based on current density, J (*3-5A/mm^2*), as follows,

$$A_{p(wire)} = \frac{I_{p(rms)}}{J} = \frac{0.71}{3} = 0.24mm^2 \tag{14}$$

The standard wire gauge (SWG) 22 is selected for this winding based on the commercial wire size present. The design of the DCM flyback converter is in discontinuous conduction mode. The maximum value of primary inductance is as follows.

$$L_{p\max} = \frac{V_{i(\min)}(t)}{I_{pr}\sqrt{2}\left(1 + \frac{V_{i(\min)}(t)}{V_R}\right) f_{sw(\min)}} = \frac{90}{1.75\sqrt{2}\left(1 + \frac{90}{150}\right) * 65000} = 350\mu H \tag{15}$$

L_{pmax} , $V_{i(min)}(t)$, I_p, and $f_{sw(min)}$ are the maximum primary winding inductance; minimum input voltage applied, the peak current through the active switch, and minimum switching frequency of converter operation. It is calculated for 90 V AC input, 65 kHz switching frequency, 150V reflection voltage, and 1.75A peak current. The maximum switching stress on the active PFC converter switch is as follows;

$$V_{ms} = V_{in(\max)} + V_R + V_{margin} = 424 + 150 + 150 = 724V \quad (16)$$

V_{ms}, $V_{in(max)}$ and V_{margin} are maximum switch voltage, maximum input voltage, and voltage margin (required for leakage inductances voltage), respectively. The MOSFET selected for this design should be calculated using Eqn. (16) for a maximum input voltage of 424V and a margin of 150V. Thus, the MOSFET of around 800V and 5A is selected for this LED driver. The secondary side current calculation is given as;

Table 1. Components used in proposed model

Parameters	Component
Bridge Rectifier	DF206ST
PFC Controller	HVLED001A
Constant Current Controller	TSM101A
Line filter	47mH and 100nF
DC bus capacitor (Cf)	470nF
Switching frequency (f_s)	65 KHz
MOSFET (M)	STP10N95K5 (800 V, 5A)
Ultrafast diode (D)	STTH3L06 (600 V, 3A)
Primary Inductance (L_{pmax})	470µH

$$I_{sr} = nI_{pr} = 1.25 * 1.75 = 2.18A \quad (17)$$

Where I_{sr} is the peak current through the diode in the secondary winding. Table 1 shows the standard selected components for flyback PFC converters.

CONTROL OF THE CONVERTER USING PWM

The LED driver is required for high brightness LED power conversion. For this, several DC-DC converters with different topologies are available. The SS flyback converter is analysed in this work because it requires fewer components than the double stage approach. The output

fixed voltage at the output, a proper feedback compensator design is required. The control feedback in projected work, and an experimental setup is used to validate the outcomes. Different PQ parameters with various line input voltages are analysed and disused in this

Figure 5. Control scheme of the Flyback converter in DCM Mode.

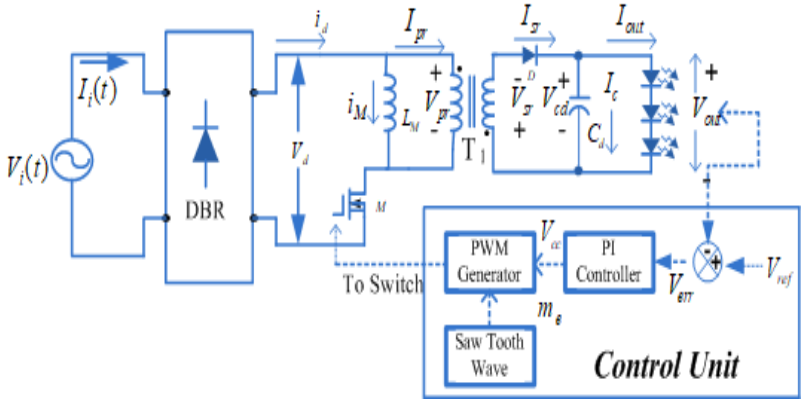

scheme of SS Configuration Flyback converter operating in DCM mode is depicted in Figure 5 to maintain fixed voltage at the output with the help of the pulse width modulation (PWM) control loop. The error signal is produced by output voltage (V_{out}) and reference voltage (V_{ref}). And the error signal is compared, which in turn generate the pulse to manage the duty cycle of the power switch and the parameters of the controller is used to regulate the voltage at the output side, and voltage error is given as (A. Shrivastava, et al., 2015),

$$V_{err}(n) = V_{ref}(n) - V_{out}(n) \tag{18}$$

And output voltage controller at nth sample instant is calculated as,

$$V_{cc}(n) = V_{cc}(n-1) + K_p\{V_{err}(n) - V_{err}(n-1)\} + K_i V_{err}(n) \quad (19)$$

Where K_p and K_i represent the integral and proportional gains, respectively. PWM generates the gate signal for the switch in order to achieve unity PF and minimise THD by comparing the high-frequency Sawtooth signal (m_e) with the output of the PI controller V_{cc}, which is given as,

$$\left\{\begin{matrix} if\, m_e < V_{cc}\, then\, Switch\, is\, 'ON' \\ if\, m_e > V_{cc}\, then\, Switch\, is\, 'OFF' \end{matrix}\right\} \quad (20)$$

EXPERIMENTAL RESULTS AND OBSERVATIONS

The performance evaluation of isolated flyback PFC fed single-stage LED driver is discussed in this section. And the experimental set-up is shown in figure 6. The PI controller is utilized as section. The operating condition for which this Flyback converter is designed; 80 Watts of power, 62 V the output voltage, 1.3 A of output current, and the switching frequency of the flyback converter is considered as 65 kHz. Table 2 shows the performance parameters of the SS Flyback converter. The maximum efficiency achieved is at 120V voltage of about 92.7% with a power factor (PF) of 0.998 and THD of 4.5%. All readings and outputs are achieved using the LED driver tester and the power analyzer. Figure 7 shows the input voltage and current at 120 V AC source, and Figure 10 shows the output current and output voltage at 120 V AC source. It indicates negligible ripples in the output voltage. Corresponding drain current and drain-source voltage are reflected in Figure 13, showing that the Flyback converter is operating in discontinuous mode. Figure 15 shows the gating pulse across the MOSFET generated by the control circuitry at a line voltage of 120 V. Table 2 indicates a high PF of 0.998, less THD of 4.5% in line current, and efficiency of 92.7 %, which satisfied the Energy Star standards. Figure 8 shows the input voltage and current at the 230 V AC source, and Figure 11 shows the output current and output voltage at the 230 V AC source. It indicates less ripples in the output voltage. Corresponding drain current and drain-source voltage are reflected in Figure 14, showing that the Flyback converter is operating in discontinuous mode. Figure 16 shows the gating pulse across the MOSFET generated by the control circuitry at a line voltage of 230 V. Table 2

indicates a high PF of 0.995, less THD in a line current is 5.2%, and efficiency of 92.1 % satisfied the Energy Star standards.

Table 2. Experimental Results of flyback converter in DCM mode

V_i (V)	I_i (mA)	V_{out} (V)	I_{out} (mA)	PF	THD (%)	P_i (Watt)	P_{out} Watt)	η (%)
120	696	61.3	1.26	0.998	4.50	83.35	77.24	92.7
230	360	61.2	1.24	0.995	5.20	82.39	75.89	92.1
270	309	61.3	1.23	0.993	6.30	82.85	75.40	91.0

Figure 9 shows the waveform of input voltage and current at 270 V AC source, and Figure 12 shows the output current and output voltage at 270 V AC source. It indicates less ripples in the output voltage. Table 2 indicates a high PF of 0.993, less THD in a line current of 6.3%, and an efficiency of 91 % satisfied the Energy Star standards.

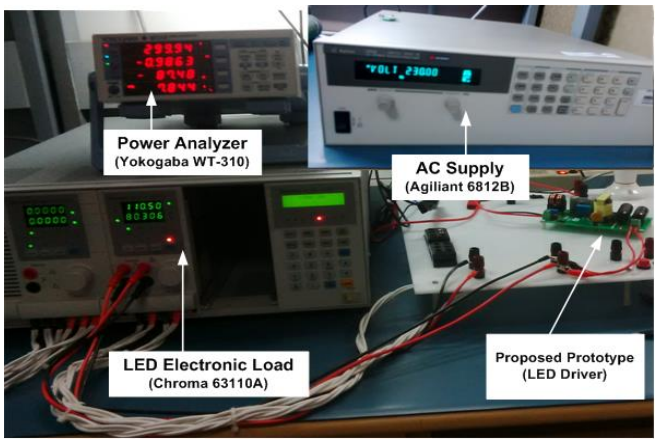

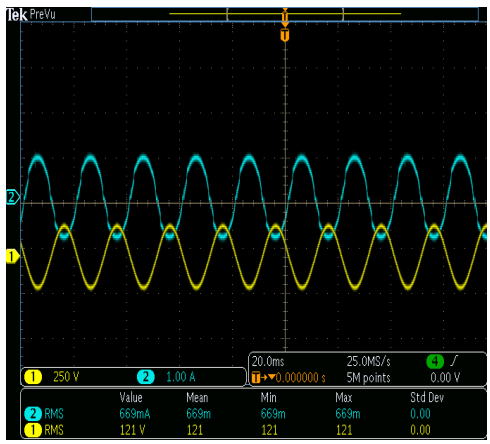

Figure 7. $V_i(t)$ and $I_i(t)$ waveform at 120 V input supply

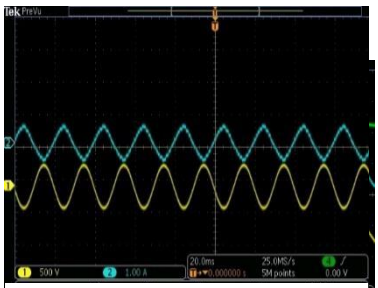

Figure 8. $V_i(t)$ and $I_i(t)$ waveform at 230 V input supply

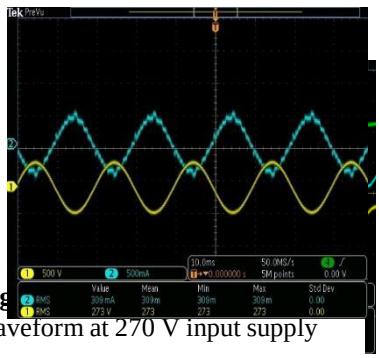

Fig waveform at 270 V input supply

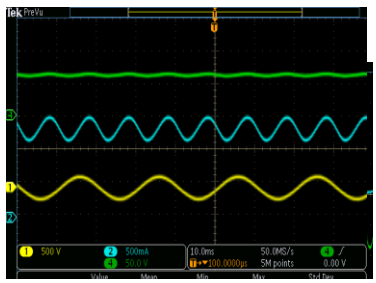

Figure 13. Drain-Source voltage and drain current at 120 V AC

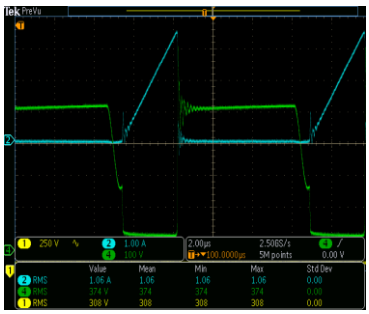

Figure 14. Drain- Source voltage and drain current at 230 V AC source

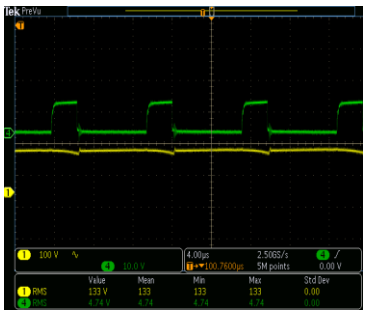

Figure 15. Gate Pulse of MOSFET at 120 V AC source

Figure 16. Gate Pulse of MOSFET 230 V AC source

CONCLUSION AND FUTURE WORK

Highly efficient LED driver circuit using DCM flyback converter with PI controller is proposed. The performance of the DCM flyback AC-DC converter is evaluated for the different universal line AC voltage level. By using PI controller for the LED driver circuit in the flyback converter, the test results show the maximum efficiency of 92.70% at 120 V AC main supplies with 0.998 power factor. Experimental results reveal the driver high power quality indices such as low THD, high efficiency and almost unity power factor achieved with the help of proposed converter and control scheme. The proposed work is the better solution for low power lighting application with low cost, high PF and high efficiency. In future the flyback-based LED driver circuit can be designed using nonlinear controllers.

REFERENCES

Y. Wang, J. M. Alonso and X. Ruan, **2017.** A Review of LED Drivers and Related Technologies, in IEEE Transactions on Industrial Electronics, vol. 64, no. 7, pp. 5754-5765, doi: 10.1109/TIE.2017.2677335.

Z. P. Da Fonseca, A. J. Perin, E. A. Junior, and C. B. Nascimento, **2017.** Single-Stage High Power Factor Converters Requiring Low DC-Link Capacitance to Drive Power LEDs, IEEE Trans. Ind. Electron., vol. 64, no. 5, pp. 3557–3567.

A. Agrawal, A. Shrivastava, and K. C. Jana, 2018. "Uniform Model and Analysis of PWM

DC-DC Converter for Discontinuous Conduction Mode," IETE J. Res., vol. 64, no. 4, pp. 569–581.

C. Y. Wu, T. F. Wu, J. R. Tsai, Y. M. Chen, and C. C. Chen, 2008. Multi string LED backlight driving system for LCD panels with color sequential display and area control, IEEE Trans. Ind. Electron., vol. 55, no. 10, pp. 3791–3800.

S. J. Choi, K. C. Lee, and B. H. Cho, 2005. Design of fluorescent lamp ballast with PFC using a power piezoelectric transformer, IEEE Trans. Ind. Electron., vol. 52, no. 6, pp. 1573–1581.

Y. Li, H. Ma, J. Xu, Q. Chen, and L. Zhang, 2018. A Single-Stage Integrated Boost-LLC AC–DC Converter with Quasi-Constant Bus Voltage for Multichannel LED Street-Lighting Applications, IEEE J. Emerg. Sel. Top. Power Electron., vol. 6, no. 3, pp. 1143–1153.

G. A. Henao, J. A. Castro, C. L. Trujillo and E. A. Narvaez, 2017. Design and development of a LED Driver prototype with a Single-Stage PFC and low current harmonic distortion, in *IEEE Latin America Transactions*, vol. 15, no. 8, pp. 1368-1375, doi: 10.1109/TLA.2017.7994781.

M. Rico-Secades, A. J. Calleja, J. Ribas, E. L. Corominas, J. M. Alonso, J. Cardesín, and J. García-García, 2005. Evaluation of a Low-Cost Permanent Emergency Lighting System Based on High-Efficiency LEDs, IEEE Transactions on Industry Applications, vol. 41, no. 5, pp.1386-1390.

Y.-L. Lin, H.-J. Chiu, Y.-K. Lo and C.-M. Leng, 2014. LED backlight driver circuit with dual-mode dimming control and current-balancing design, IEEE Trans. Ind. Electron., vol. 61, no. 9, pp. 4632–4639.

B. Singh, B. N. Singh, A. Chandra, K. Al-Haddad, A. Pandey and D. P. Kothari, 2003. A review of single-phase improved power quality AC-DC converters, in *IEEE Transactions on Industrial Electronics*, vol. 50, no. 5, pp. 962-981, doi: 10.1109/TIE.2003.817609.

Singh, B., Singh, S., Chandra, A., Al-Haddad, K., 2011. Comprehensive study of single-phase AC–DC power factor corrected converters with high-frequency isolation, IEEE Trans. Ind. Inf., 7, (4), pp. 540–556.

Deo. Rajesh, Shrivastava, A. and Chatterjee, Kalyan, 2019. Single Stage Isolated Zeta Converter (SS-IZC) Circuit with Improved Power Factor for LED's Application. IOP

Conference Series: Materials Science and Engineering. 594. 012014.

Yongqiang Zheng; Moschopoulos G., 2006. Design considerations for a new ac-dc single-stage flyback converter, APEC'2006.

C.-A. Cheng, C.-H. Chang, T.-Y. Chung and F. L. Yang, 2015. Design and implementation of a single-stage driver for supplying an LED street-lighting module with power factor corrections, IEEE Trans. Power Electron., vol. 30, no. 2, pp. 956–966.

H. H. Chou, Y. S. Hwang, and J. J. Chen, 2013. An adaptive output current estimation circuit for a primary-side controlled LED driver, IEEE Trans. Power Electron., vol. 28, no. 10, pp. 4811–4819.

J. M. Zhang, H. L. Zeng and T. Jiang, 2012. A primary-side control scheme for high-power-factor LED driver with TRIAC dimming capability, IEEE Trans. Power Electron., vol. 27, no. 11, pp. 4619–4629.

X. G. Xie, J. Wang, C. Zhao, Q. Lu, and S. R. Liu, 2012. A novel output current estimation and regulation circuit for primary side controlled high power factor single-stage flyback LED driver, IEEE Trans. Power Electron., vol. 27, no. 11, pp. 4602–4612.

J. T. Hwang, M. S. Jung, D. H. Kim, J. H. Lee, M. H. Jung, and J. H. Shin, 2012. Off-the-line primary side regulation LED lamp driver with single- stage PFC FLYBACK and TRIAC dimming using LED forward voltage and duty variation tracking control, IEEE J. Solid-State Circuits, vol. 47, no. 12, pp. 3081–3094.

P.-C. Hsieh, C.-J. Chang, and C.-L. Chen, 2013. A primary-side- control quasi-resonant flyback converter with tight output volt- age regulation and self-calibrated valley switching, in Proc. IEEE Energy Conv. Congr. Expo. (ECCE), Denver, CO, USA, pp. 3406–3412.

A. Shrivastava, B. Singh, and S. Pal, 2015. A Novel Wall-Switched Step-Dimming Concept in LED Lighting Systems Using PFC Zeta Converter, IEEE Trans. Ind. Electron., vol. 62, no. 10, pp. 6272–6283.